Spectral properties and magneto-optical excitations in semiconductor double rings under Rashba spin-orbit interaction

Wen-Hsuan Kuan,[1] Chi-Shung Tang,[2] and Cheng-Hung Chang[1,3]
[1]*Physics Division, National Center for Theoretical Sciences, Hsinchu 30013, Taiwan, Republic of China*
[2]*Research Center for Applied Sciences, Academia Sinica, Taipei 11529, Taiwan, Republic of China*
[3]*Institute of Physics, National Chiao Tung University, Hsinchu 30013, Taiwan, Republic of China*
(Received 13 September 2006; revised manuscript received 6 January 2007; published 23 April 2007)

We have numerically solved the Hamiltonian of an electron in a semiconductor double ring subjected to the magnetic flux and Rashba spin-orbit interaction. It is found that the Aharonov-Bohm energy spectrum reveals multizigzag periodic structures. The investigations of spin-dependent electron dynamics via Rabi oscillations in two-level and three-level systems demonstrate the possibility of manipulating quantum states. Our results show that the optimal control of photon-assisted inter-ring transitions can be achieved by employing cascade-type and Λ-type transition mechanisms. Under chirped pulse impulsions, a robust and complete transfer of an electron to the final state is shown to coincide with the estimation of the Landau-Zener formula.

DOI: 10.1103/PhysRevB.75.155326 PACS number(s): 74.25.Gz, 71.70.Ej, 74.25.Nf

I. INTRODUCTION

The progress in epitaxial growth promotes the use of low-dimensional semiconductor nanostructures in optoelectronic devices. Investigations on fundamental physical properties such as the electronic structure and the carrier population can be directly measured and estimated from the photoluminescence spectrum. Theoretically, several proposals on magneto-optical studies for quantum dot systems have been put forward in the last decade.[1] Nowadays, coherent optical manipulations of single quantum systems have attracted further attention. The mature technologies in optical control and measurements provide a great opportunity to realize quantum qubits as logical gates[2] in storage and quantum information processing.[3]

In the 1990s, the progress of technology has enabled the experimental study of a mesoscopic ring threaded by a static magnetic-field display persistent currents,[4,5] which oscillate as a function of magnetic flux Φ with a period $\Phi_0=hc/e$. Recently, applications on spin-orbit interaction (SOI) originated from the breaking of inversion symmetry that gives rise to intrinsic spin splitting in semiconductor systems open a field of spintronics. It was pointed out that the quantum transport of electrons in a spin-polarized system differs greatly from that in a spin-degenerate device.[6] The utilization of the spin degree of freedom offers the mechanism to speed up quantum information processing. In nature electronic devices such as the Datta-Das transistor,[7] spin waveguide[8] and spin filter[9] were proposed.

Several theoretical works associated with Rashba SOI due to structural inversion asymmetry in quantum dot systems were studied.[10] More recently, the success in self-assembled formation of concentric quantum double rings[11] provides a new system to explore electron dynamics by magneto-optical excitations on the basis of fully analyzed signature of Aharonov-Bohm (AB) spectrum within the effect of Rashba SOI. The radius of flat double rings is about 100 nm with thickness of approximately 3 nm. Therefore, carriers are coherent all throughout these small geometries. Within a time scale shorter than the dephasing time,[12] the Rabi oscillation (RO) can provide a direct control of excited state population especially in strong excitation regime. It was proposed to be a good optical implement in quantum dot systems.[13] However, a simple two-level system involving Rabi oscillations with Rashba SOI in a coaxial double quantum ring has not yet been studied. Therefore, in this paper, we consider two-level and three-level models to explore spin-dependent electron dynamics assisted by RO processes. Under the influence of magnetic flux, the spin feature of the system is demonstrated only through the effects of Rashba SOI. The presence of Rashba SOI also plays an important role in the mixture of neighboring angular momenta as well as spins that build up a new selection rule, and it opens more dipole-allowed transition routes.

In view of quantum algorithm realization, the two-level Rabi oscillators are often the prototype of the quibit generators. However, it is also important to establish coherent control in realistic multilevel quantum systems.[14,15] Hence, we explore the multilevel dynamical system involving the cascade-type and the Λ-type three-level schemes driven by either sinusoidal impulsions or chirped laser pulses. To achieve efficient transfers, we employ adiabatic rapid passage method (ARP),[16,17] namely, that the excitation process rapid compared with the natural lifetime of an excited state in the limit of slowly varying detuning field, to simulate complete transfer processes. We will show that the probability of an electron that occupies the final state coincides with the estimation of the Landau-Zener formula in the adiabatic limit.[18]

The paper is organized as follows. In Sec. II, the single-particle Hamiltonian is derived and numerically solved and SOI accompanied AB energy spectrum is analyzed. In Sec. III, ROs between two levels selected from the double-ring spectrum are studied. In Sec. IV, photon-assisted electron transitions in the three-level systems of the cascade and Λ schemes are investigated. Finally, the paper ends with a conclusion in Sec. V.

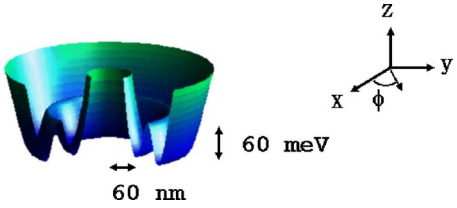

FIG. 1. (Color online) The diagram of part of the double-ring potential depicted in $0 \leqslant \phi \leqslant 3\pi/2$. The radius of the ring is about 160 nm and effective range of the magnetic flux r_Φ is about 7 nm.

II. THE ENERGY SPECTRA OF THE DOUBLE-RING SYSTEM

The system of a double-ring two-dimensional electron gas is enclosed by a magnetic flux in the presence of Rashba SOI. The electron is confined in an axial-symmetric potential V_c, shown in Fig. 1, which is exposed in a monochromatic electromagnetic (EM) field. In semiclassical description, the Hamiltonian is given by

$$H = \frac{1}{2m^*}\left[\vec{p} - \frac{e}{c}\mathbf{A}(\vec{r},t)\right]^2 + V_c(r) + \frac{\alpha}{\hbar}\left\{\vec{\sigma} \times \left[\vec{p} - \frac{e}{c}\mathbf{A}(\vec{r},t)\right]\right\}_z, \tag{1}$$

where $\mathbf{A}(\vec{r},t)$ contains contributions from the magnetic flux and the EM field and α is the coupling constant of Rashba SOI. The double-ring potential is modeled as

$$V_c(r) = \frac{1}{2}m^*\omega_0^2(r - r_0)^2 + \sum_{i=1}^{3} V_i e^{-(r-r_i)^2/\sigma_i^2}, \tag{2}$$

where ω_0 is a factor defining the characteristic length $l_c = \sqrt{\hbar/m^*\omega_0}$ of the system and σ_i is the Gaussian spatial width. The magnetic flux applied through the central region of the inner ring within r_Φ is described by the vector potential $\vec{A}_\Phi = Br/2\hat{\phi}$ for $r \leqslant r_\Phi$ and $\vec{A}_\Phi = Br_\Phi^2/2r\hat{\phi}$ for $r > r_\Phi$. Therein, the unit vector in the angular direction $\hat{\phi} = -\sin(\phi)\hat{x} + \cos(\phi)\hat{y}$ has been used. The effect of the linearly polarized EM wave is simply expressed as $\vec{\mathcal{A}}_{EM}(t) = A_0 \sin(kz - \Omega t)\hat{x}$, where k and Ω are the wave vector and the frequency of the wave.

The Hamiltonian can be divided as $H = H_0 + H_{\text{int}}$, where H_0 and H_{int} correspond to the unperturbed and time-dependent Hamiltonians, respectively. From energy conservation, the rapidly oscillating quadratic term in $\vec{\mathcal{A}}_{EM}(t)$ is omitted, and hence

$$H_{\text{int}} \simeq -\left[\frac{e\vec{\mathcal{A}}_{EM}}{m^*c}\left(\vec{p} - \frac{e}{c}\vec{A}_\Phi\right) + \frac{\alpha e}{\hbar c}[\vec{\sigma} \times \vec{\mathcal{A}}_{EM}]_z\right]. \tag{3}$$

It is convenient to rewrite $H_{\text{int}} = H_D + H_B + H_{SO}$, indicating three different types of interaction. The first term is the electron dipole interaction, given by

$$H_D = \frac{-e}{m^*c}\vec{\mathcal{A}}_{EM} \cdot \vec{p} \simeq -e\vec{x} \cdot \vec{E}, \tag{4}$$

where the time-dependent electric field, $\vec{E} = \mathcal{E}_0 \cos(\Omega t)\hat{x}$, is polarized along the **x** direction. The second contribution H_B is due to the applied magnetic flux,

$$H_B = \frac{e^2}{m^{*}c^2}\vec{\mathcal{A}}_{EM} \cdot \vec{A}_\Phi = \frac{e^2\mathcal{E}_0}{m^*c\Omega}A_\Phi(r)\sin(\phi)\sin(\Omega t). \tag{5}$$

The third term H_{SO} denotes the SO coupling mechanism,

$$H_{SO} = -\frac{\alpha e}{\hbar c}(\vec{\sigma} \times \vec{\mathcal{A}}_{EM})_z = \frac{-\alpha e\mathcal{E}_0}{\hbar\Omega}\sigma_y \sin(\Omega t). \tag{6}$$

The electron dynamics can be derived based on the knowledge of eigenfunctions of H_0. At $t=0$, the normalized two-component wave function is $\Psi = (\Psi_\uparrow, \Psi_\downarrow)^T$, where

$$\Psi_\sigma = \psi_\sigma(\vec{r}) \otimes \chi_\sigma, \tag{7}$$

with $\sigma = \uparrow$ or $\downarrow$ indicating two spin branches. Since total angular momentum J_z commutes with time-independent Hamiltonian in the presence of SOI, the spatial wave function can be expressed in the form

$$\psi_\uparrow(\vec{r}) = \psi_{l_\uparrow}(r)e^{il_\uparrow\phi},$$

$$\psi_\downarrow(\vec{r}) = \psi_{l_\downarrow}(r)e^{il_\downarrow\phi}, \tag{8}$$

where the orbital angular momenta $l_\uparrow = m_j - 1/2$ and $l_\downarrow = m_j + 1/2$ follow the relation $l_\downarrow = l_\uparrow + 1$, with m_j corresponding to the eigenvalue of J_z. While dipole interaction does not flip spin directly, the spin flipping is possibly achieved in the presence of the SOI, and therefore we can investigate the spin-dependent charge dynamics. To characterize this feature, we define the net spin polarizability

$$\mathcal{P} = \frac{\langle\Psi|\sigma_z|\Psi\rangle}{\langle\Psi|\Psi\rangle} = \frac{\langle\Psi_\uparrow|\Psi_\uparrow\rangle - \langle\Psi_\downarrow|\Psi_\downarrow\rangle}{\langle\Psi|\Psi\rangle}. \tag{9}$$

For the case of $|\mathcal{P}| = 1$, this indicates that the system is totally polarized into spin $\uparrow$ (spin $\downarrow$) if $\mathcal{P} = +1$ ($\mathcal{P} = -1$). Otherwise, the spin polarizability can be generally specified by the notation $\mathcal{P}_\uparrow$ if $\mathcal{P} > 0$ and $\mathcal{P}_\downarrow$ if $\mathcal{P} < 0$.

Specifically, we consider an InAs-based double quantum ring system, of which the quantum structures are appropriate to investigate some spin-related phenomena.[19] Below, we have selected the InAs material parameters $m^*/m_0 = 0.042$ and $\alpha \sim 40$ meV nm. Correspondingly, the characteristic energy $E = \hbar\omega_0 = 5$ meV and for the EM field $\hbar\Omega = 1$ meV. The dimensionless parameters of the double-ring potential are

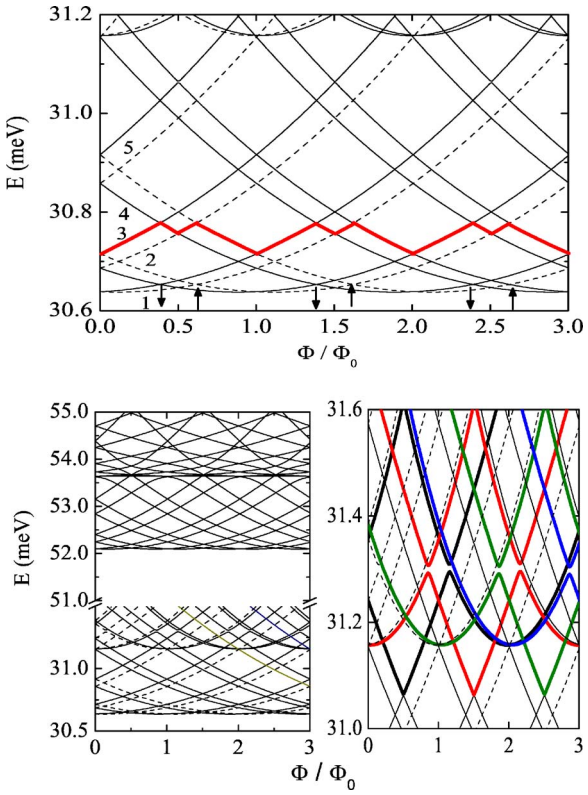

FIG. 2. (Color online) (a) The Aharonov-Bohm oscillations in the energy spectrum of the double ring in the presence of the Rashba SOI with α=40 meV nm and a static magnetic flux. The spectrum of states with positive (negative) m_j is depicted in solid (dashed) curves. The lowest five pairs of the states are specified by $|m_j|$=2.5, 3.5, 1.5, 4.5, and 0.5. In each $1/2-\Phi/\Phi_0$ region, up or down arrows denote net spin orientations of ground states. The zigzag curve shows the sixth lowest eigenenergy. (b) Energy levels within lowest four subbands, in which energies of subband bottoms line close by 30.6, 31.2, 52.1, and 53.6 meV, respectively. (c) Near the second subband bottom, anticrossing levels are depicted in thick curves. From left to right, these states are of m_j=0.5, 2.5, 1.5, and 3.5.

r_c=0, V_1=70, V_2=20, V_3=−20, σ_1=1.825, σ_2=1.0, σ_3=2.236, r_1=0, r_2=5.0, and r_3=6.0. In the numerical calculation, we shall present the magnetic flux in units of the flux quantum $\Phi_0=hc/e$.

By choosing the above typical physical quantities and diagonalizing the time-independent Hamiltonian, it is easy to obtain the single-particle energy spectrum, as shown in Fig. 2(a). As compared with the energy spectra in usual quantum dots, a genuine effect of SOI can be revealed in the reduction of degeneracies from fourfold to at most twofold. However, for rings there are only twofold degeneracies at zero magnetic flux whether the SOI exists or not. The presence of the magnetic flux breaks the time reversal symmetry but Kramer's degeneracy is not lifted due to the absence of the Zeeman effect. In Fig. 2(a), the solid curves indicate energy levels of positive m_j, whereas those of negative m_j are depicted by dashed curves. The lowest five pairs of energy levels belong to $|m_j|$=2.5, 3.5, 1.5, 4.5, and 0.5. The ordering of these levels could change if the coupling constant α of the Rashba SOI is varied. For instance, when α=5 meV nm, the lowest five pairs of these levels are with $|m_j|$=0.5, 1.5, 0.5, 2.5, and 1.5. In the concern of varying α, one can drive coherent ROs and the idea has been realized in quantum dot systems.[20]

In the absence of the magnetic flux, the second and the third (as well as the fourth, the fifth, etc.) levels in Fig. 2(a) are close to each other. The gap between these adjacent levels arises from the zero-field splitting of the Rashba SOI, which will disappear when the SOI coupling constant α approaches zero. In the limit $\alpha\to 0$, not only the adjacent levels at $\Phi/\Phi_0=0$ mentioned above but also the curves split from these levels in the region $\Phi/\Phi_0>0$ will merge together. Another decisive feature distinguishing quantum rings from quantum dots stands out that for the former the ground state will periodically shift to that of higher total angular momentum. However, it always corresponds to the state with the lowest angular momentum in quantum dots.

An energy level E in Fig. 2(a) is a piecewise smooth function of Φ/Φ_0 with singular crossing points. The zigzag thick curve shows an example of the sixth lowest level, which has five crossing points around Φ/Φ_0=0.5, 0.6, 1.0, 1.4, and 1.5 within the unit interval $0.5<\Phi/\Phi_0<1.5$ at α=40 meV nm. If $\alpha\to 0$, the pairs of curves merge as discussed above and the set of crossing points reduce to Φ/Φ_0=0.5 and 1.5 for the ground state, and reduce to Φ/Φ_0=0.5, 1.0, and 1.5 for other levels. It turns out that at α=0, the electron in the double-ring reveals a similar oscillation pattern, with the same oscillation period one, as the AB oscillations in a single ring without SOI.[21,22] For $\alpha>0$, the splitting of local spin branches in AB oscillating spectrum of a single ring can be identified.[23] For the double ring, spectral patterns become more complicated, but patterns with regular oscillations are still rather apparent. Moreover, the spin polarizability $\mathcal{P}$ defined in Eq. (9) varies in Φ/Φ_0. It seems that the crossing points of the lowest level in Fig. 2(a), i.e., at $\Phi/\Phi_0=\{0.5,1,1.5,2,\ldots\}$, are exactly the positions where $\mathcal{P}$ changes its sign, at least in the range we studied.

To explain the location of the crossing points in Fig. 2(a), let us consider an ideal one-dimensional ring of radius R enclosing a magnetic flux. The spectral property of this system reflects some key features of a radial subband of the double ring [Fig. 2(b)]. The flux-dependent energy spectrum can be derived in the analytical form,

$$E=\frac{\hbar\omega_a}{2}\left\{\left(l_\uparrow-\frac{\Phi}{\Phi_0}\right)^2+\left(l_\downarrow-\frac{\Phi}{\Phi_0}\right)^2\pm\sqrt{\left[\left(l_\uparrow-\frac{\Phi}{\Phi_0}\right)^2-\left(l_\downarrow-\frac{\Phi}{\Phi_0}\right)^2\right]^2+\frac{4\alpha^2}{R^2}\frac{1}{\hbar^2\omega_a^2}\left(l_\uparrow-\frac{\Phi}{\Phi_0}\right)\left(l_\downarrow-\frac{\Phi}{\Phi_0}\right)}\right\},\tag{10}$$

where $\hbar\omega_a=\hbar^2/2m^*R^2$. Due to the relation $l_\downarrow=l_\uparrow+1$, the energy E can be expressed as a function of the variables $l_\downarrow$ and Φ/Φ_0. A crossing point will come up at a certain Φ/Φ_0 where different integers $l_\downarrow$ have the same energy E. According to Eq. (10), this happens when Φ increases from zero to a period Φ_0 if the Rashba SOI is absent. In the presence of the Rashba SOI, additional crossing points appear before Φ reaches Φ_0. As compared to the Fock-Darwin spectrum in a quantum dot where the energy is in linear proportion to the trapping frequency and the cyclotron frequency in weak and strong magnetic fields, respectively. However, while SOI can be regarded as the perturbation, Eq. (10) tells well a quadratic relation with the magnetic flux.

Level crossing points can be easily seen in Fig. 2(a). Anticrossing levels also appear, for instance, in the example of Fig. 2(c), and even in high-energy regimes, as seen in the two dashed lines at $(\Phi/\Phi_0,E)=(1.7,53.7)$ in Fig. 4(a). While the splitting of the accidental level degeneracy in quantum dots has been demonstrated both theoretically and experimentally,[24] the repulsions in the avoiding levels due to the interplay between Zeeman and Rashba terms are also reported recently.[25] In our case, anticrossings near the second subband bottom arise in the presence of strong SOI. However, for high-energy pairs, the repulsions here are mainly attributed to the geometric effect of the double ring under the influence of magnetic flux. In other words, the repulsion levels in the double ring will not disappear, even when Rashba effect is turned off. In the vicinity of the minimal splitting points, wave functions vary acutely and cannot be specified by a set of good quantum numbers. The double-ring Hamiltonian thus typically manifests the signature of quantum chaos. A comparison between the spectra of $\alpha=0$ and 20 meV nm shows that the Rashba SOI will increase the level splitting in each energy pair mentioned above but decrease the gap of the repulsion levels from 0.32 to 0.28 meV. Moreover, by adiabatically modulating the gate voltage to change SOI, the double-ring system discussed here serves as a candidate for testing the Berry phase.[26]

III. RABI OSCILLATIONS IN TWO-LEVEL TRANSITIONS

Since an electron in the inner (outer) ring has a definite angular momentum, its tunneling probability to the neighbor ring is suppressed under the constraint of the angular momentum conservation. Therefore, an eigenfunction in the double ring may be localized only in the inner or the outer ring, if its corresponding energy is lower than the barrier. In the following, we are going to investigate the dynamics of an electron under irradiations of an external EM field in the presence of SOI. The transition between two such kind of quantized levels in the energy space corresponds to an inter-ring transition in the spatial space.

We consider arbitrarily two levels in the double ring. Suppose the electron initially occupies state $|b\rangle$ with eigenfunction $u_b(\vec{r})$ in the outer ring, the irradiation process is designed to pump it to state $|a\rangle$ with eigenfunction $u_a(\vec{r})$ in the inner ring. For convenience, the time-dependent wave function can be written as

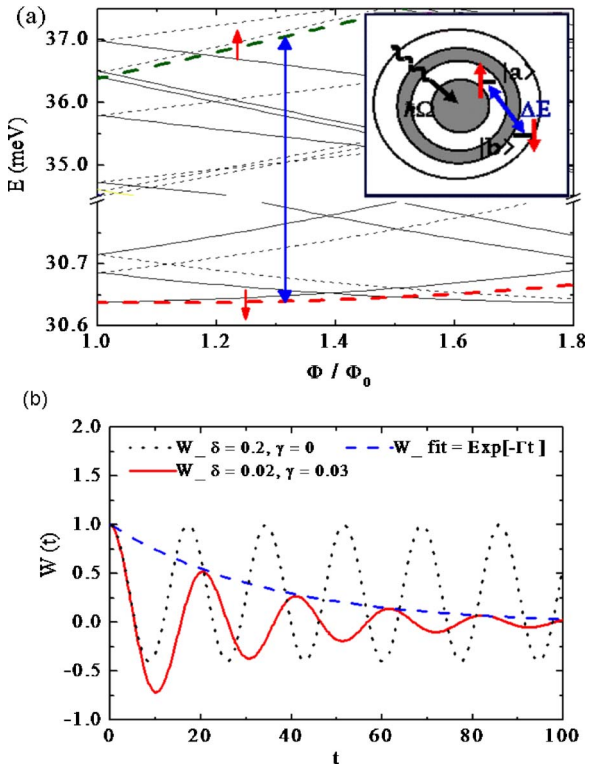

FIG. 3. (Color online) (a) The energy spectrum including two states: $|a\rangle=|-2.5\rangle_{\mathcal{P}_\uparrow}$ and $|b\rangle=|-1.5\rangle_{\mathcal{P}_\downarrow}$. The sketch in the inset depicts inter-ring transitions under EM wave stimulations. (b) Population inversion as a function of time. When ignoring the spontaneous emission, $W(t)$ with large detuning is demonstrated by dotted symbol. If the spontaneous emission of an excited state is considered, then in small detuning regime, where we set $\gamma=0.03$ and $\delta=0.02$, $W(t)$ manifests an underdamped oscillation, as depicted by the solid curve, and the decay behavior is fitted by an exponential decay function, as shown by the dashed line.

$$\psi(\vec{r},t)=c_a(t)e^{i(\delta/2-\omega_a)t}u_a(\vec{r})+c_b(t)e^{i(-\delta/2-\omega_b)t}u_b(\vec{r}), \quad (11)$$

where $u_a(\vec{r})$ and $u_b(\vec{r})$ associated with $E_j=\hbar\omega_j$ for $j=a$ and b, related to the two-component wave function Ψ in Eq. (7), as eigenfunctions and eigenenergies of H_0. Moreover, an optical transition takes place between two states that correspond to dipole-allowed eigenstates conforming to the relation $\Delta m_j=\pm 1$. As usual, $\delta\equiv(\Delta E/\hbar-\Omega)$ is the detuning defined as the frequency difference between the level spacing and the laser field, as shown in the inset of Fig. 3(a). Inserting Eq. (11) into the time-dependent Schrödinger equation, the time evolution of an electron can be expressed as

$$\begin{bmatrix}\dot{c}_a(t)\\ \dot{c}_b(t)\end{bmatrix}=\frac{i}{2}\begin{bmatrix}-\delta & R_D+\tilde{R}\\ R_D^*+\tilde{R}^* & \delta\end{bmatrix}\begin{bmatrix}c_a(t)\\ c_b(t)\end{bmatrix}, \quad (12)$$

with $\tilde{R}=R_A+R_{SO}$, which after some calculations have the relations

$$R_D = e\mathcal{E}_0\langle u_a(r)|r|u_b(r)\rangle/4\hbar,$$

$$R_B = e^2\mathcal{E}_0\langle u_a(r)|A_\Phi(r)|u_b(r)\rangle/4\hbar m^* c\Omega,$$

$$R_{SO} = \alpha e\mathcal{E}_0\langle u_a(r)|u_b(r)\rangle/2\hbar^2\Omega.$$

Therein, R_D is the dipole-induced Rabi frequency as usually discussed and R_B and R_{SO} denote the couplings of the laser field with the magnetic flux and the Rashba SOI, respectively. In calculating R_{SO}, only inner products between partial waves with different spin orientations would be taken into account. In deriving Eq. (12), we utilized the rotating-wave approximation (RWA) and ignored the counter-rotating terms proportional to $\exp[\pm i(\Omega+\Delta E/\hbar)t]$.

For an electron initially occupying the low-energy state $|b\rangle$, the time-dependent population probability can be exactly written as

$$|c_a|^2 = \frac{\tilde{R}_{\text{eff}}^2}{\Omega_d^2}\sin^2\left(\frac{\Omega_d t}{2}\right),$$

$$|c_b|^2 = 1 - \frac{\tilde{R}_{\text{eff}}^2}{\Omega_d^2}\sin^2\left(\frac{\Omega_d t}{2}\right), \tag{13}$$

where $\Omega_d^2=\tilde{R}_{\text{eff}}^2+\delta^2$ and $\tilde{R}_{\text{eff}}=R_D+\tilde{R}$ can be regarded as the *effective Rabi frequency* in the presence of the external fields and the SOI. The on-resonance transitions occur when $\delta=0$; in the case, the population probability can be simply reduced to $|c_a|^2=\sin^2(\tilde{R}_{\text{eff}}t/2)$ and $|c_b|^2=\cos^2(\tilde{R}_{\text{eff}}t/2)$.

If the energy dissipation to the environment is considered as the interaction between an electron with continuous vacuum modes, a phenomenological decay parameter γ will be introduced to the first element of the matrix in Eq. (12), which opens a decay path from the excited state to its surrounding. Thus, the coefficients describing the system will be changed in the more complicated form,

$$|c_a|^2 = \frac{\tilde{R}_{\text{eff}}^2}{\tilde{\Omega}^2}e^{-\gamma t}e^{-\tilde{\Omega}\zeta t}\sin^2\left(\frac{\tilde{\Omega}\eta t}{2}\right),$$

$$|c_b|^2 = \frac{e^{-\gamma t}}{\tilde{\Omega}^2}e^{-\tilde{\Omega}\zeta t}\left[(\gamma^2+\delta^2)\sin^2\left(\frac{\tilde{\Omega}\eta t}{2}\right) + \tilde{\Omega}^2\cos^2\left(\frac{\tilde{\Omega}\eta t}{2}\right) + 2\tilde{\Omega}(\gamma\eta - |\delta|\zeta)\sin(\tilde{\Omega}\eta t)\right], \tag{14}$$

where $\zeta=\cos(\theta_1/2)$ and $\eta=\sin(\theta_2/2)$, with

$$\theta_1 = \cos^{-1}[(\gamma^2-\Omega_d^2)/\tilde{\Omega}^2],$$

$$\theta_2 = \sin^{-1}[2|\delta|\gamma/\tilde{\Omega}^2],$$

$$\tilde{\Omega}^2 = \sqrt{(\gamma^2-\Omega_d^2)^2+(2\delta\gamma)^2},$$

in which θ_1 and θ_2 should be taken from the same quadrant.

For convenience, we introduce the notation $|m_j\rangle_{\mathcal{P}}$ to specify a state in terms of the total angular momentum m_j and its spin polarizability $\mathcal{P}$. We choose two states $|a\rangle=|-2.5\rangle_{\mathcal{P}_\uparrow}$ and $|b\rangle=|-1.5\rangle_{\mathcal{P}_\downarrow}$, respectively, at $\Phi=1.3\Phi_0$ with $E_a=37.03$ meV and $E_b=30.64$ meV, as depicted in Fig. 3(a). The corresponding population inversion

$$W(t) = |c_b(t)|^2 - |c_a(t)|^2 \tag{15}$$

of this system is demonstrated in Fig. 3(b). If the vacuum fluctuation is absent ($\gamma=0$), the total probability is conserved, i.e., $|c_b(t)|^2+|c_a(t)|^2=1$ at any time. In this case, $W(t)$ manifests the oscillating behavior within the interval $[1-2(\tilde{R}_{\text{eff}}^2/\Omega_d^2),1]$ without any dissipation. For $\delta\to 0$, this interval approaches to its maximum values $[-1,1]$, namely, that $\Omega_d\to\tilde{R}_{\text{eff}}$. For large detuning, e.g., $\delta=0.2$, this interval will shrink to its 70%, and the blueshifted inversion curve is plotted in the dotted line in Fig. 3(b).

If the spontaneous emission of an excited state is considered, $W(t)$ will decay with time, as shown by the solid curve in Fig. 3(b), in which $\gamma=0.03$ and $\delta=0.02$. In this case, $W(t)$ oscillates underdamped. The damping behavior which is consistent with the Weisskopf-Wigner theory[27] is well fitted by $W_{\text{fit}}=e^{-\Gamma t}$, where the Fermi's rate $\Gamma\sim 0.03$. When the Rabi relaxation time is defined as $\tau_R=1/\Gamma$, our calculation shows that a cycle of inter-ring transition accomplishes in τ_R for a given γ. While the spontaneous decay can be experimentally controlled and suppressed,[28] in a cavity with a limited number of modes at the transition frequency, a long decoherence time is permitted. In assumption of weak system-environment coupling, efficient population transfers are feasible. So, in conclusion, under SOI we can simultaneously manipulate electron transitions associated with its spin orientations in either rings via the RO processes of a two-level model.

IV. THE PHOTON-ASSISTED TRANSITIONS IN THREE-LEVEL SCHEMES

In this section, we apply the Rabi model to several interesting cases. We show how inter-ring transition are achieved via the photon-assisted processes. The processes are demonstrated by considering three-level systems in cascade-type and Λ-type schemes that are shown in Figs 4(a) and 4(b). For clarity, we rewrite the time-dependent wave function as $\psi(\vec{r},t)=\Sigma_{j=1}^3 c_j(t)e^{-i\omega_j t}u_j(\vec{r})$, where $E_j=\hbar\omega_j$ and we define $E_{12}=E_2-E_1$, $E_{13}=E_3-E_1$ and $E_{12}+\delta=E_{13}-\delta=\hbar\Omega$. The involved states construct two dipole-allowed transitions $\{|1\rangle\leftrightarrow|2\rangle\}$ and $\{|1\rangle\leftrightarrow|3\rangle\}$ and a $\{|2\rangle\leftrightarrow|3\rangle\}$ dipole-forbidden paths. For a clear demonstration, we shall ignore spontaneous emission processes.

A. Cascade type

It is well known that the quantum-beat spectroscopic method permits the resolution of closely neighboring levels.[29] Earlier experiments demonstrate that quantum-beat spectroscopy is a useful technique in the measurement of Zeeman splittings and hyperfine intervals in atomic and molecular systems.[30] It is then interesting to study spectroscopic dynamics involving the *direct* inter-ring transitions in the

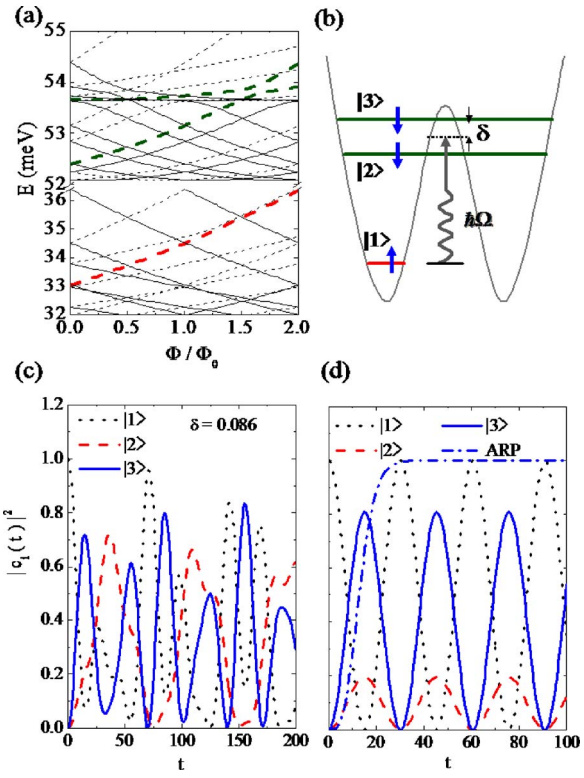

FIG. 4. (Color online) (a) The energy spectrum including the chosen three levels, an up-spin state $|1\rangle=|-1.5\rangle_{\mathcal{P}_\uparrow}$ and down-spin doublets $|2\rangle=|-2.5\rangle_{\mathcal{P}_\downarrow}$ and $|3\rangle=|-2.5\rangle_{\mathcal{P}_\downarrow}$ at $\Phi=1.7\Phi_0$. Level repulsion occurs between the doublets, and the gap is about 0.17 meV for $\alpha=40$ meV nm. (b) A sketch of a cascade-type model in the double ring population as a function of time for the cases of (c) $\delta=0.086$ and (d) $\delta\to 0$. Dash-dotted curve in (d) shows the ARP estimation of the transition from $|2\rangle$ to $|3\rangle$.

cascade-type scheme nearby the avoided crossing points.

Again, we use the notation $|m_j\rangle_{\mathcal{P}}$ to specify the involving states. Here, we consider an up-spin state $|1\rangle=|-1.5\rangle_{\mathcal{P}_\uparrow}$, and down-spin doublets $|2\rangle=|-2.5\rangle_{\mathcal{P}_\downarrow}$ and $|3\rangle=|-2.5\rangle_{\mathcal{P}_\downarrow}$ at $\Phi=1.7\Phi_0$. For state $|1\rangle$, the electron is localized in the inner ring. The electron wave functions, however, extend over the double ring for two higher states. The energy spectrum is depicted in Fig. 4(a), and in Fig. 4(b) we show the sketch of the cascade model. Similar to solving Eq. (12) for the two-level system, transitions among different spin states can be investigated through

$$\dot{c}_1(t)=\frac{i}{2}[e^{-i\delta t}R_+^{12}c_2(t)+e^{i\delta t}R_-^{13}c_3(t)],$$

$$\dot{c}_2(t)=\frac{i}{2}e^{i\delta t}R_+^{*21}c_1(t),$$

$$\dot{c}_3(t)=\frac{i}{2}e^{-i\delta t}R_-^{*31}c_1(t), \tag{16}$$

where $R_\pm^{ij}=R_D^{ij}\pm\tilde{R}^{ij}$. Adopting transformations $c_2(t)=C_2(t)e^{i\delta t}$ and $c_3(t)=C_3(t)e^{-i\delta t}$, Eq. (16) can be reexpressed as a homogeneous autonomous equation. For an electron initially occupying state $|1\rangle$, the population probability in small detuning regime can be expressed approximately as

$$|c_1(t)|^2=\cos^2\left(\frac{M_R t}{2}\right),$$

$$|c_2(t)|^2=\left(\frac{R_+^{12}}{M_R}\right)^2\sin^2\left(\frac{M_R t}{2}\right),$$

$$|c_3(t)|^2=\left(\frac{R_-^{13}}{M_R}\right)^2\sin^2\left(\frac{M_R t}{2}\right), \tag{17}$$

where $M_R=\sqrt{(R_+^{12})^2+(R_-^{13})^2}$. Beyond the small detuning approximation, Eq. (16) is numerically solved and the result for $\delta=0.086$ is shown in Fig. 4(c). Since transition probabilities come up differently between two paths, namely, $R_+^{12}\neq R_-^{13}$, occupations with time on each states turn out to be aperiodic and less regular compared with probabilities obtained from Eq. (17). Discrepancies between Figs. 4(c) and 4(d) are clearly illustrated. However, in the case $\delta\to 0$, the electron tends to oscillate between $|3\rangle$ and $|1\rangle$ and the transition $|2\rangle\leftrightarrow|3\rangle$ is less efficient, as compared with the off-resonance transitions.

This drawback can be removed by another interesting manipulation in the cascade scheme, namely, by transferring electrons ladder by ladder with chirped laser pulses. The idea originates from the electron transfer in molecules, in which stepwise excitations are applied for a rapid and efficient dissociation of specific chemical bonds.[31] Under ARP condition, electrons that are resonantly pumped to state $|2\rangle$ could be efficiently transited to the final state $|3\rangle$ in a long trapping time.

To this end, we select a chirped laser pulse with time-dependent electric field along the radial direction, given by

$$\vec{\mathcal{E}}_{ch}(t)=\mathcal{E}_{ch}\exp\left(-\frac{t^2}{2\tau^2}-i\Omega_{ch}t-i\beta\frac{t^2}{2}\right)\hat{r}, \tag{18}$$

where τ is the pulse duration, Ω_{ch} is the central frequency, and β is the temporal chirp. The equation of motion in RWA modified from Eq. (12) becomes

$$\begin{bmatrix}\dot{c}_2(t)\\ \dot{c}_3(t)\end{bmatrix}=\frac{i}{2}\begin{bmatrix}0 & R_{ch}(t)\\ R_{ch}^*(t) & 2\delta_{ch}(t)\end{bmatrix}\begin{bmatrix}c_2(t)\\ c_3(t)\end{bmatrix}, \tag{19}$$

in which $\delta_{ch}(t)=\beta t$ is linearly chirped detuning, and $R_{ch}(t)$ stands for the time-dependent Rabi frequency related to the pulse envelope of $\vec{\mathcal{E}}_{ch}(t)$. By choosing proper parameters for a pulse with peak Rabi frequency $R_0=0.25$, $\beta=0.01$, and $\tau=10$, a complete transfer is demonstrated by the dash-dotted line in Fig. 4(d). The numerical result coincides with the estimation of the Landau-Zener formula,[18]

$$P\simeq 1-\exp\left(-\pi\frac{R_0^2}{2\beta}\right). \tag{20}$$

In the adiabatic limit $|\beta|\ll R_0^2$, electrons have great probability to occupy an excited state in the long-time limit. Distinguished time-evolution populations between stimulated transitions by cws and steady transfer by a chirp pulse are

depicted by curves in Fig. 4(d). Therefore, in addition to the manipulation of electron transitions between a single ring and a double ring via the subjection to cw irradiations, we also arrive at the optimal control on stably selective excitations with chirped pulses in cascade-type systems.

B. Λ-type transition

Finally, we shall also investigate an interesting and important phenomenon: Whenever there are level crossings for two energy states that belong to either one ring, Λ-type scheme of indirect inter-ring transitions among which and one higher energy state can be switched on. Applications of this model has been proposed both in superconducting quantum interference device[33] and semiconductor double quantum dots,[34] in which multilevel ROs as a target toward coherent control have been demonstrated.

As Fig. 5(a) shows that for an electron occupying state $|2\rangle$, the photon-assisted quantum transition is initiated from the inter-ring surpassing an intermediate-state $|1\rangle$ and finally reaching the outer-ring of state $|3\rangle$. On-resonance solutions of the *mediated-indirect-transition* system with initial conditions $c_1(0)=0$, $c_2(0)=1$, and $c_3(0)=0$ are

$$|c_1(t)|^2 = \left(\frac{R_+^{12}}{M_R}\right)^2 \sin^2\left(\frac{M_R t}{2}\right),$$

$$|c_2(t)|^2 = \left(\frac{R_+^{12}}{M_R}\right)^4 \cos^2\left(\frac{M_R t}{2}\right) + \left(\frac{R_-^{13}}{M_R}\right)^4 + \frac{2(R_+^{12}R_-^{13})^2}{M_R^4}\cos\left(\frac{M_R t}{2}\right),$$

$$|c_3(t)|^2 = \frac{(R_+^{12}R_-^{13})^2}{M_R^4}\left[\cos\left(\frac{M_R t}{2}\right) - 1\right]^2, \qquad (21)$$

and the transition probabilities are shown in Fig. 4(b). The incomplete transfer and occupation are restricted due to unequal effective Rabi frequencies in two paths. Once the external field optimizes the efficiency of one path, the efficiency of the other is not optimal.

The formulas in Eq. (21) clearly show that the probability $|c_3(t)|^2$ has a maximum value at $t=m\pi/M_R$ with an odd integer m and a minimum value at $t=n\pi/M_R$ with an even integer n. At these extreme points, we have the ratio $|c_2(t)|^2/|c_3(t)|^2=[(R_+^{12})^2-(R_-^{13})^2]^2/4(R_+^{12})^2(R_-^{13})^2$, which indicates the optimal transfer at $|R_+^{12}|/|R_-^{13}|=1$. Away from this ratio, the transfer efficiency will decrease. In Fig. 4(b), transition among a doublet of $m_j=0.5$ and 2.5 and an auxiliary level of $m_j=1.5$ at $\Phi=0.8\Phi_0$ is considered. In this case, there is only 45% occupation in $|3\rangle$ for $R_+^{12}/R_-^{13}\sim 0.38$. If the effective Rabi frequencies of the paths $2\leftrightarrow 1$ and $1\leftrightarrow 3$ are the same, the optimal control of electron dynamics is feasible. To show this, we calculate the time-dependent occupation probability in each state. In the inset, it is clear that at extreme times, occupation in $|3\rangle$ based on a pseudo-Λ-transition process has a maximum value. Meanwhile, states $|1\rangle$ and $|2\rangle$ are left empty. Moreover, we also investigate the transition process stimulated by chirped pulse irradiation. By setting R_0

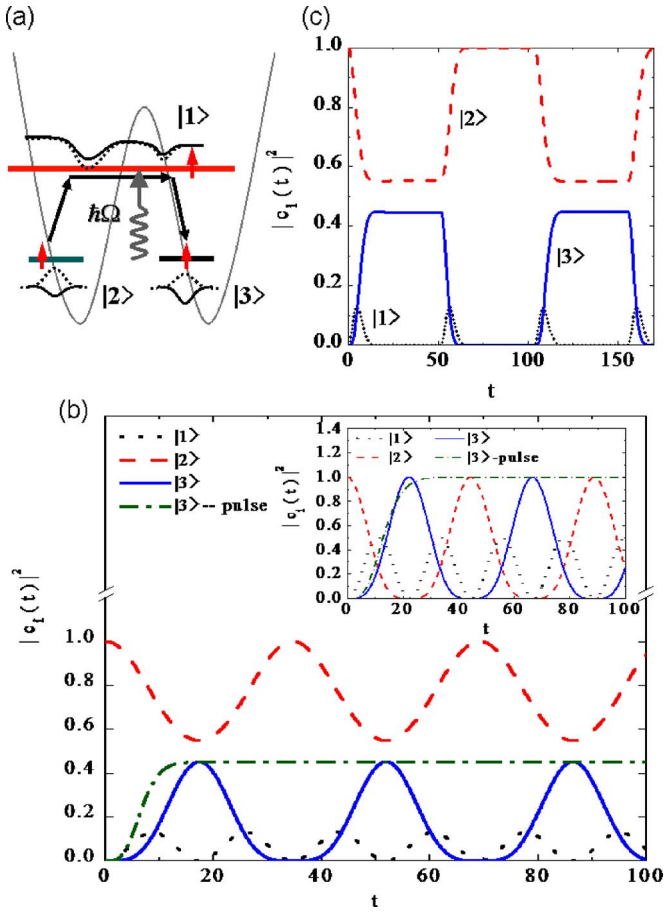

FIG. 5. (Color online) (a) A sketch of the Λ-type scheme. States here are all with effective up-spin orientations. An electron initially occupies state $|2\rangle$ can be optically pumped to an outer-ring state $|3\rangle$ mediated by state $|1\rangle$. (b) The population probabilities among three levels. The long-time occupation of an excited state is feasible by applying a short and intense pulse. In the inset, we show the optimal transfer is feasible provided that there is common Rabi frequency in the two paths. (c) An alternative output signal can be obtained under successive pulse stimulations.

$=0.25$, $\beta=0.001$, and $\tau=14.15$, we obtain a long-time occupation of the final state, obeying estimation of Landau-Zener's formula. The result is shown by dash-dotted line in the inset.

Within proper controls of the pulse width τ against the typical level spacings and the dephasing time of electrons, it is easy to manipulate electronic states in Λ-scheme system by successive application of pulses.[32] Using the same parameters as in Fig. 4(b), we simulate the pulse-induced periodic oscillations. Here, the Gaussian pulse duration $\tau=7.3$ and the pulse interval is about 7τ. Different from the sinusoidal ROs, an alternative square wave is shown in Fig. 4(c). Apparently, the level occupation time in both inner and outer rings is prolonged. Moreover, since the duration of the pulse is properly tuned, it can be expected that time evolution of the occupation should be complete in the pseudo-Λ-transition process. Otherwise, underexcitation or overexcitation takes place corresponding to the duration being too short or too long, respectively. Level occupation will never be or just be

transiently complete. The well controled pulse delay time also shows the flexibility of manipulations in quantum states.

V. CONCLUSION

In this work, we have studied magneto-optical transitions in a semiconductor double ring in the presence of Rashba spin-orbit coupling and magnetic flux. First, based on accurate numerical calculations, we obtain SOI-accompanied AB energy spectra and corresponding eigenstates. The presence of the SOI has important influence on the occurrence of level crossings, showing the evidence both for the periodic orbital motion and for spin flips. In addition, there are anticrossing levels playing the role of the magnetic-resonant extraditions of electrons between inner and outer rings. In high-energy regime, occurrence of avoided crossings indicates a chaotic signature in its classical analogy. To facilitate the peculiar features of the double-ring system, we have designed some interesting dynamic processes such that the system can be easily explored experimentally in the near future.

We have studied the temporal evolution processes in two-level and two three-level models. The interaction between external fields and electron results in the successive stimulating absorption and emission of a photon and turns out as the effective Rabi oscillators. In the two-level model, we demonstrate an alternative manipulation of electrons transiting between two rings. In cascade scheme, aperiodic and incomplete population transfers are revealed under the sinusoidal field excitations. By appropriate tuning SOI strength, the gap between avoided crossing levels can be reduced such that the rectified output signals are measurable. Moreover, by short pulse excitations, we also demonstrate the possibility of optimal control of selective and direct signals. In this work, only one ladder transition is demonstrated, which, however, can be extended to multiladder transitions following the same principle. Finally, we have explored the photon-assisted tunneling in the Λ-type model. In addition to generation of ROs also, we give the criterion of the most efficient transfer via the mediated-indirect-tunneling paths. Further, by successive pulse irradiations, the well control on pulse delay results in the time prolongation on state populations. We should also emphasize that in the Λ-type scheme, the minimization of the intermediate-level population is achieved which is an important and practical strategy in device realization.

The presence of SOI allows the manipulation of spin degree of freedom and it is timely to examine the spin-dependent optical response. Since similar features could be found in double-dot systems, the above theoretical results in a double ring might shed light on future experimental findings in these burgeoning quantum systems. While there are few works on optically induced and SOI-driven spin dynamics in quantum systems,[20,35,36] we believe that the theoretical and experimental works of related spin readout information by optical pumping in ringlike systems could be carried out in the near future.

ACKNOWLEDGMENTS

This work was supported by National Science Council and Academia Sinica in Taiwan. The authors are grateful for valuable discussions with V. Gudmundsson, Y. N. Chen, G. Y. Chen, and W. Xu.

[1] P. A. Maksym and T. Chakraborty, Phys. Rev. Lett. **65**, 108 (1990); T. Chakraborty, Comments Condens. Matter Phys. **16**, 35 (1992); T. Chakraborty, *Quantum Dots* (North-Holland, Amsterdam, 1999); I. Magnusdottir and V. Gudmundsson, Phys. Rev. B **60**, 16591 (1999); R. Krahne, V. Gudmundsson, C. Heyn, and D. Heitmann, *ibid.* **63**, 195303 (2001).

[2] J. Gorman, E. G. Emiroglu, D. G. Hasko, and D. A. Williams, Phys. Rev. Lett. **95**, 090502 (2005); T. Hayashi, T. Fujisawa, H. D. Cheong, Y. H. Jeong, and Y. Hirayama, *ibid.* **91**, 226804 (2003); X. Li, Y. Wu, D. Steel, D. Garmon, T. H. Stievater, D. S. Katzer, D. Park, C. Oiermarocchi, and L. J. Sham, Science **301**, 809 (2003).

[3] B. E. Kane, Nature (London) **393**, 133 (1998); M. Friesen, C. Tahan, R. Joynt, and M. A. Eriksson, Phys. Rev. Lett. **92**, 037901 (2004); E. Paspalakis, Z. Kis, E. Voutsinas, and A. F. Terzis, Phys. Rev. B **69**, 155316 (2004).

[4] L. P. Levy, G. Dolan, J. Dunsmuir, and H. Bouchiat, Phys. Rev. Lett. **64**, 2074 (1990).

[5] V. Chandrasekhar, R. A. Webb, M. J. Brady, M. B. Ketchen, W. J. Gallagher, and A. Kleinsasser, Phys. Rev. Lett. **67**, 3578 (1991).

[6] I. Zutic, J. Fabian, and S. Das Sarma, Rev. Mod. Phys. **76**, 323 (2004).

[7] B. Datta and S. Das, Appl. Phys. Lett. **56**, 665 (1990).

[8] X. F. Wang, P. Vasilopoulos, and F. M. Peeters, Phys. Rev. B **65**, 165217 (2002).

[9] T. Koga, J. Nitta, H. Takayanagi, and S. Datta, Phys. Rev. Lett. **88**, 126601 (2002).

[10] W. H. Kuan, C. S. Tang, and W. Xu, J. Appl. Phys. **95**, 6368 (2004); O. Voskoboynikov, C. P. Lee, and O. Tretyak, Phys. Rev. B **63**, 165306 (2001); M. Valin-Rodriguez, A. Puente, and L. Serra, *ibid.* **69**, 085306 (2004); S. Debald and C. Emary, Phys. Rev. Lett. **94**, 226803 (2005).

[11] T. Mano, T. Kuroda, S. Sanguinetti, T. Ochiai, T. Tateno, J. Kim, T. Noda, M. Kawabe, K. Sakoda, G. Kido, and N. Koguchi, Nano Lett. **5**, 425 (2005).

[12] L. Allen and J. H. Eberly, *Optical Resonance and Two-Level Atoms* (Dover, New York, 1987).

[13] H. Kamada, H. Gotoh, J. Temmyo, T. Takagahara, and H. Ando, Phys. Rev. Lett. **87**, 246401 (2001); T. H. Stievater, Xiaoqin Li, D. G. Steel, D. Gammon, D. S. Katzer, D. Park, C. Piermarocchi, and L. J. Sham, *ibid.* **87**, 133603 (2001); H. Htoon, T. Takagahara, D. Kulik, O. Baklenov, A. L. Holmes, Jr., and C. K. Shih, *ibid.* **88**, 087401 (2002); P. Borri, W. Langbein, S. Schneider, U. Woggon, R. L. Sellin, D. Ouyang, and D. Bimberg, Phys. Rev. B **66**, 081306(R) (2002); S. Stufler, P. Ester, A. Zrenner, and M. Bichler, *ibid.* **72**, 121301(R) (2005).

[14] W. S. Warren, H. Rabitz, and M. Dahleh, Science **259**, 1581 (1993); J. L. Krause and R. M. Whitnell, K. R. Wilson, and Y. J.

Yan, in *Femtosecond Chemistry*, edited by J. Manz and L. Wöste (VCH, Weinheim, 1995), pp. 743–779; S. A. Rice and M. Zhao, *Optical Control of Molecular Dynamics* (Wiley, New York, NY, 2000).

[15] S. Chelkowski, A. D. Bandrauk, and P. B. Corkum, Phys. Rev. Lett. **65**, 2355 (1990); J. S. Melinger, D. McMorrow, C. Hillegas, and W. S. Warren, Phys. Rev. A **51**, 3366 (1995); M. N. Kobrak and S. A. Rice, *ibid.* **57**, 2885 (1998).

[16] J. S. Melinger, S. R. Gandhi, A. Hariharan, D. Goswami, and W. S. Warren, J. Chem. Phys. **101**, 6439 (1994); V. S. Malinovsky and J. L. Krause, Eur. Phys. J. D **14**, 147 (2001).

[17] C. W. Hillegas, J. X. Tull, D. Goswami, D. Strickland, and W. S. Warren, Opt. Lett. **19**, 737 (1994); M. M. Wefers and K. A. Nelson, *ibid.* **18**, 2032 (1993).

[18] L. D. Landau, Phys. Z. Sowjetunion **2**, 46 (1932); C. Zener, Proc. R. Soc. London, Ser. A **137**, 696 (1932).

[19] D. Grundler, Phys. Rev. Lett. **84**, 6074 (2000); C.-M. Hu, J. Nitta, T. Akazaki, H. Takayanagi, J. Osaka, P. Pfeffer, and W. Zawadzki, Physica E (Amsterdam) **6**, 767 (2000).

[20] S. Debald and C. Emary, Phys. Rev. Lett. **94**, 226803 (2005).

[21] A. Führer, S. Luscher, T. Ihn, T. Henzel, K. Ensslin, W. Wegsheider, and M. Bichler, Nature (London) **413**, 822 (2001); A. Lorke, R. J. Luyken, A. O. Govorov, J. P. Kotthaus, J. M. Garcia, and P. M. Petroff, Phys. Rev. Lett. **84**, 2223 (2000).

[22] T. Chakraborty and P. Pietiläinen, Phys. Rev. B **50**, 8460 (1994); P. Pietiläinen and T. Chakraborty, *ibid.* **73**, 155315 (2006).

[23] J. Splettstoesser, M. Governale, and U. Zülicke, Phys. Rev. B **68**, 165341 (2003).

[24] B. Jouault, G. Santoro, and A. Tagliacozzo, Phys. Rev. B **61**, 10242 (2000); L. P. Kouwenhoven, T. H. Oosterkamp, M. W. S. Danoesastro, M. Eto, D. G. Austing, T. Honda, and S. Tarucha, Science **278**, 1788 (1997).

[25] T. Chakraborty and P. Pietiläinen, Phys. Rev. Lett. **95**, 136603 (2005).

[26] D. Giuliano, P. Sodano, and A. Tagliacozzo, Phys. Rev. B **67**, 155317 (2003); S.-R. Eric Yang and N. Y. Hwang, *ibid.* **73**, 125330 (2006).

[27] *Methods in Theoretical Quantum Optics*, edited by S. Barnett and P. Radmore (Clarendon, Oxford, 1997), Chap. 5.

[28] E. M. Purcell, Phys. Rev. **69**, 681 (1946); E. Yablonovitch, Phys. Rev. Lett. **58**, 2059 (1987); H. Hirayama, T. Hamano, and Y. Aoyagi, Appl. Phys. Lett. **69**, 791 (1996).

[29] *The Physics of Atoms and Quanta*, edited by H. Haken and H. Wolf (Springer, New York, 1996), pp. 386–388.

[30] S. Haroche, M. Gross, and M. P. Silverman, Phys. Rev. Lett. **28**, 1063 (1974); R. Wallenstein, J. A. Paisner, and A. L. Schawlow, *ibid.* **32**, 1333 (1974).

[31] S. Chelkowski and G. N. Gibson, Phys. Rev. A **52**, R3417 (1995); D. J. Maas, C. W. Rella, P. Antoine, E. S. Toma, and L. D. Noordam, *ibid.* **59**, 1374 (1999).

[32] R. Gómez-Abal and W. Hübner, Phys. Rev. B **65**, 195114 (2002).

[33] Z. Zhou, Shih-I. Chu, and S. Han, Phys. Rev. B **66**, 054527 (2002).

[34] A. V. Tsukanov, Phys. Rev. B **73**, 085308 (2006).

[35] F. T. Vasko, Phys. Rev. B **70**, 073305 (2004); A. Y. Smirnov and L. G. Mourokh, *ibid.* **71**, 161305(R) (2005).

[36] F. Malet, M. Pi, M. Barranco, E. Lipparini, and Ll. Serra, Phys. Rev. B **74**, 193309 (2006).